North Pacific–North Atlantic relationships under stratospheric control?

J. M. Castanheira
Department of Physics, University of Aveiro, Aveiro, Portugal

H.-F. Graf
Max-Planck Institute for Meteorology, Hamburg, Germany

Received 12 July 2002; revised 11 September 2002; accepted 13 September 2002; published 15 January 2003.

[1] Based on a linear regression/correlation analysis of monthly mean atmospheric sea level pressure (SLP) data from the National Centers for Environmental Prediction (NCEP) reanalysis (1948–2000), we find a significant anticorrelation between pressure in the northern North Atlantic and North Pacific only if the stratospheric circulation is in the "strong polar vortex" regime but not when the vortex is weak. Since some general circulation models (GCMs) (e.g., European Center/Hamburg (ECHAM4)) are biased toward the strong vortex regime (SVR), they tend to reproduce this anticorrelation already in the mean. The pattern of the "Arctic Oscillation" (AO) is shown to be consistent with the mean surface pressure differences between the two stratospheric regimes. The typical SW-NE tilt of the node line of the North Atlantic Oscillation (NAO) found with linear analyses (i.e., with such that do not take the regime character of the stratospheric circulation into account) in Northern Hemisphere winter is due to a superposition of correlation patterns based on physical processes working in the troposphere (a strictly meridional dipole and the pattern resulting from planetary wave refraction in the strong vortex regime) and those produced by the rapid transition from one stratospheric regime to the other with subsequent downward propagation of the signal. This result underlines the necessity of the application of nonlinear statistics or the restriction of linear statistics to variations in the stable (quasi-linear) environment of natural regimes. *INDEX TERMS:* 3309 Meteorology and Atmospheric Dynamics: Climatology (1620); 3319 Meteorology and Atmospheric Dynamics: General circulation; 3362 Meteorology and Atmospheric Dynamics: Stratosphere/troposphere interactions; 3384 Meteorology and Atmospheric Dynamics: Waves and tides; *KEYWORDS:* North Atlantic Oscillation, annular modes

Citation: Castanheira, J. M., and H.-F. Graf, North Pacific–North Atlantic relationships under stratospheric control?, *J. Geophys. Res.*, *108*(D1), 4036, doi:10.1029/2002JD002754, 2003.

1. Introduction

[2] After decades of relative silence, the North Atlantic Oscillation (NAO) and its significance for the Eurasian weather and climate is enjoying a renaissance. However, even today the fundamental mechanisms of this important variability mode of the Northern Hemisphere climate seem to be understood only incompletely and large research programs and conferences give this phenomenon high priority.

[3] The NAO, either based on simple indices like the anomalous pressure difference of the two centers of action involved, the Azores High and the Icelandic Low, or on more sophisticated methods like Empirical Orthogonal Functions (EOFs) in the North Atlantic sector, is claimed to be quite well reproduced by the current climate models (atmospheric models alone [*Barnett*, 1985; *Glowienka-Hense*, 1990], coupled ocean–atmosphere models [*Paeth et al.*, 1999]) and, if the sea surface temperature (SST) is prescribed as observed during the last century, also part of the historic behavior of a low-pass filtered NAO index can be reproduced [*Rodwell et al.*, 1999; *Latif et al.*, 2000]. However, if the whole Northern Hemisphere is included in the analysis, certain differences between the models and observations appear mainly in the relationships between the North Pacific and the North Atlantic. *Osborn et al.* [1999, Figure 3] studied the behavior of the Hadley Centre's coupled climate model (HadCM2) in terms of its simulation of the NAO. In the simulated data, they found significant correlation between the atmospheric circulation over the North Pacific and an index of the NAO, while no signal was apparent in the observations. In another climate model (European Center/Hamburg (ECHAM3)), *May and Bengtsson* [1998] found similar results and U. Ulbrich and M. Christoph (Mechanisms of the PNA influence on the NAO, submitted to *Climate Dynamics*, 2002, hereinafter referred to as Ulbrich and Christoph, submitted manuscript, 2002) found statistically significant correlation between the NAO and PNA

0148-0227/03/2002JD002754

indices as simulated by the general circulation model (GCM) ECHAM4/OPYC3. Again, there is clearly missing evidence for any such significant relationship in observations. Only *Honda et al.* [2001] found a highly significant anticorrelation between the Aleutian and the Icelandic lows in NCEP reanalysis data from the years 1973–1994, which is restricted to late winter, February–March. *Deser* [2000] and *Ambaum et al.* [2001] presented clear evidence that, even though leading EOFs of the atmospheric pressure fields show structures which would suggest a connection between the North Pacific and the North Atlantic, the local variables are not statistically significantly correlated. However, all these studies made no separation between months with lower stratospheric winds above or below critical Rossby velocities. Hence, a possible impact of the strength of the high latitude northern polar vortex was ignored.

[4] A large fraction of climate variability may be due to transitions between different circulation regimes, and these transitions may encompass nonlinear processes [e.g., *Corti et al.*, 1999; *Palmer*, 1999; *Perlwitz et al.*, 2000; *Monahan et al.*, 2001] (A. H. Monahan et al., The vertical structure of wintertime climate regimes of the Northern Hemisphere extratropical atmosphere, submitted to *Journal of Climate*, 2001, hereinafter referred to as Monahan et al., submitted manuscript, 2001). An example of such nonlinear processes is the upward propagation or downward reflection of planetary waves depending on the strength of the westerlies in the lower extratropical stratosphere in winter [*Charney and Drazin*, 1961]. Under certain approximations, if the zonal mean wind is westerly and smaller than the wave number and latitude dependent critical Rossby velocity, planetary waves can further propagate upward, otherwise they are reflected and modify the tropospheric flow. In the case of a strong polar night vortex this can lead to a significant change of mid tropospheric geopotential patterns few days later [*Perlwitz and Graf*, 2001a], while there is no significant lag correlation from stratospheric to tropospheric circulation during a weak vortex episode. Since some climate models [*Pawson et al.*, 2000; *Hein et al.*, 2001] tend to overestimate the stratospheric zonal wind in winter on the Northern Hemisphere, the simulated circulation may have greater probability to be in a regime different from the preferred regime of the observed natural system, and the simulated response to external forcing (e.g., greenhouse gases, volcanic aerosols, and solar and ozone changes) may result in other anomaly patterns and/or amplitudes than observed [*Perlwitz et al.*, 2000]. To see if the results of the above mentioned models may be attributed to a model bias resulting from the too strong polar vortex, and the results of *Honda et al.* [2001] are due to the very strong polar vortex in late winter (mainly during the years they included in their data set) we performed a correlation/regression analysis on a monthly basis divided into months with either observed strong or weak zonal winds in the lower stratosphere. We consider an extended cool season from November to April as used by *Thompson and Wallace* [1998], *Corti et al.* [1999], and *Deser* [2000].

2. Data and Data Preparation

[5] The data were obtained from the National Centers for Environmental Prediction (NCEP) reanalysis data set [*Kalnay et al.*, 1996]. We used the wintertime (November–April) monthly means of sea level pressure (SLP) and zonal wind at 50 hPa with a horizontal grid resolution of 2.5° lat. × 2.5° long., north of 20°N, covering the period 1948–2000. The seasonal cycle of the SLP fields was removed by subtracting the long-term mean of each month. Next, we detrended the data by subtraction of the 5 year running mean at each grid point. This way we reduce the influence of possible data inhomogeneities on time series analysis and exclude decadal variability that may be due to external (e.g., SST) forcing. However, it must be noted that the main results of this work are not sensitive to the detrending. We constructed three sets of detrended data: The first including all detrended data from 1951 to 1998 (288 months). A second set includes only the months when $0 < \overline{u}_{50}(65°\text{N}) < 10$ m s^{-1}, where $\overline{u}_{50}(65°\text{N})$ is the 50 hPa zonal mean zonal wind at 65°N. We consider this the Weak Vortex Regime (WVR, 72 months). A third one including only the months when $\overline{u}_{50}(65°\text{N}) > 20$ m s^{-1}. We consider this the Strong Vortex Regime (SVR, 87 months). The wind was not detrended and the seasonal cycle was not removed. We explicitly exclude polar warming events with zonal mean easterly winds.

Table 1. Case Numbers of WVR ($0 < \overline{u}_{50}(65°\text{N}) < 10$ m s^{-1}) and SVR ($\overline{u}_{50}(65°\text{N}) > 20$ m s^{-1}) for Each Month of the Cool Season (November–April)

	N	D	J	F	M	A	Total
			WVR				
1951–1974	4	3	2	5	9	17	40
1975–1998	2	2	1	2	9	16	32
All Period	6	5	3	7	18	33	72
			SVR				
1951–1974	1	9	13	11	4	0	38
1975–1998	2	13	16	12	5	1	49
All Period	3	22	29	23	9	1	87

[6] Table 1 shows the number of months selected as SVR or WVR during the boreal cold season (November–April). Clearly, SVR is concentrated to the main winter months (DJF), while the WVR most frequently occurs during the late winter/early spring (March and April). We checked if the WVR results possibly may be determined by the large number of cases in April by repeating the analyses without the April data and found no evidence for this. We also repeated the analysis by just separating between SVR and non-SVR months (i.e., westerlies weaker than 20 m s^{-1}) and found similar results as the ones discussed later as well for the extended winter periods as for the main winter months DJF.

[7] The regime thresholds are somewhat arbitrary for the real atmosphere, but reflect critical Rossby velocities (20 m s^{-1}) for zonal wave number (ZWN) 1 near the polar circle for a climatological North Hemispheric zonal wind profile (meridional index of 1, wind speed increasing to the midstratosphere) [*Andrews et al.*, 1987]. In this case, planetary wave disturbances of the northern polar vortex in the middle stratosphere are excluded and the polar vortex may develop undisturbed toward the radiative equilibrium. The limit for the WVR (westwind, <10 m s^{-1}) allows all energetically important planetary waves (i.e., those with ZWN1–3) to propagate vertically.

[8] For a realistic atmosphere, linear wave propagation depends on the ZWN as well as on the meridional and vertical profiles and magnitude of background winds. As suggested by *Hu and Tung* [2002], the strength of the polar night jet plays a major role for wave refraction in the NCEP reanalysis. Since exact critical velocities cannot be found, we need to find a compromise here for the separation of the regimes. With the limits defined, we can be sure that in the SVR at least much less ultralong planetary wave activity propagates into the stratosphere than in the WVR. This may be concluded from Figure 1, which shows the Eliassen–Palm (EP) flux composite differences for SVR, non-SVR, and WVR periods.

[9] The EP flux was calculated using its quasi-geostrophic version in spherical geometry [*Andrews et al.*, 1987, equation (5.2.6)]. In order to view the EP flux throughout the stratosphere, the vectors were scaled by $\sqrt{p_0/p}$, with p_0 = 1000 hPa [*Randel et al.*, 1987]. Additionally, the vertical component was multiplied by 125.

[10] To compute EP flux composites we considered an SVR episode if the daily $\overline{u}_{50}$(65°N) is above 20 m s^{-1} during 30 consecutive days at least. The non-SVR and WVR episodes were identified as the periods where the 17 days running mean of $\overline{u}_{50}$(65°N) is below 20 and 10 m s^{-1}, respectively, during 30 consecutive days at least. Warming episodes leading to negative running mean were excluded. We chose the episodes to have a minimum duration of 30 days because our data stratification for analysis of SLP field is based on monthly means of $\overline{u}_{50}$(65°N). For SVR, we found many episodes for which the daily $\overline{u}_{50}$(65°N) remains above 20 m s^{-1} longer than 30 days. For non-SVR and WVR, we found only a few cases where the daily u_{50}(65°N) remains below 20 and 10 m s^{-1}, respectively, during 30 days at least. As was shown by *Perlwitz and Graf* [2001a], in the SVR, tropospheric planetary waves of ZWN1 will influence the stratospheric circulation and this acts back on the troposphere, the whole process taking about 8–10 days. Then we chose a half window of 8 days for the running mean, i.e., the minimum time interval for the complete troposphere–stratosphere interaction under SVR. In order to preclude problems with seasonality, and as more SVR than WVR episodes were found, we chose a subset of SVR episodes with seasonal distribution similar to that of WVR. Obviously, non-SVRs may include WVRs.

[11] The EP fluxes of waves 1 + 2 + 3 for SVR, WVR and their difference (not shown) are very close to the respective EP fluxes and difference for high and low Northern Hemisphere Annular Mode (NAM) indices computed by *Hartmann et al.* [2000]. The EP flux vectors in the upper troposphere and lower stratosphere bend more equatorward during SVR periods, indicating that planetary waves are bent away from the polar vortex when it is strong. Since the wave refraction depends of its wave number, in Figure 1, we show the EP flux composite differences for individual waves s = 1 and 2. During SVR episodes, an increased equatorward energy propagation is observed for both wave numbers, at latitudes north of 50°N. A reduced vertical energy propagation of zonal wave s = 1 in the high latitude stratosphere is also observed. Thus, the chosen thresholds for $\overline{u}_{50}$(65°N) imply clear differences on ultra long planetary wave refraction in the NCEP reanalysis.

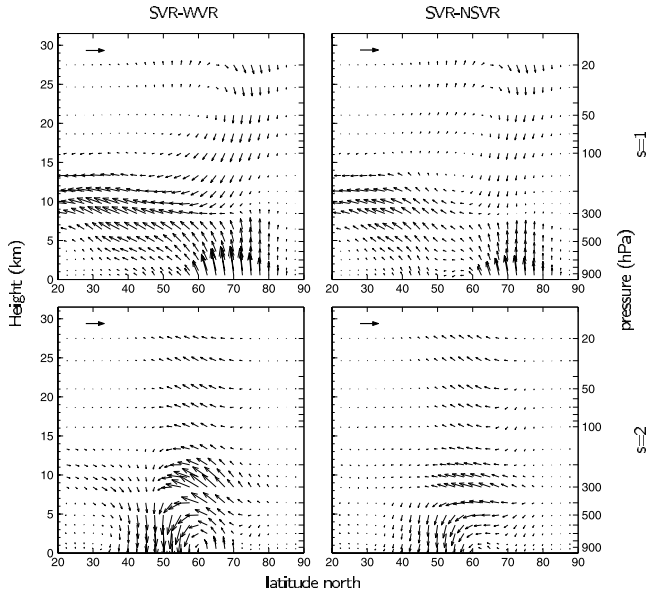

Figure 1. EP flux composite differences of individual waves s = 1 and 2 for SVR, NSVR, and WVR. The vector at the upper left corner represents $3a\rho_0(0)$ m^2 s^{-2} of the scaled EP flux.

[12] We further constructed indices of the NAO, the strength of the Azores High and of the Icelandic Low. The NAO index is simply the difference of the SLP normalized to their standard deviation of the grid points closest to Ponta Delgada (Azores) and Reykjavik (Iceland). The Azores High index is the mean of the four data points of SLP closest to Ponta Delgada, and the Icelandic Low index is the mean of the four data points closest to Reykjavik.

3. Results

[13] For each of the three data sets (all data, weak and strong polar vortex) we computed the regression (isolines)/correlation (shading) maps of the SLP upon the NAO index (Figures 2 and 3). The regression values are in hPa per one standard deviation of the above defined NAO index. The standard deviation has been calculated for each case. It is 1.79, 1.97, and 1.57 for all data, SVR, and WVR, respectively.

[14] In all three cases the dominant role of the North Atlantic pressure seesaw is evident as expected. Figure 2 is coherent with a similar analysis of observed data by *Osborn et al.* [1999]. However, there are significant differences between the WVR (Figure 3, left) and the SVR (Figure 3, right) mainly over the North Pacific. The SLP in the western part of the Aleutian Low is positively correlated with the NAO index (r_{max} = 0.39) under SVR conditions. A remainder of this signal is seen in Figure 2 for all data. We adopted a threshold for shading of 0.1 for the correlation in the case of all data (288 months), and the threshold of 0.2 for the WVR (73 months) and SVR (87 months). The two thresholds are statistically significant at the 95% confidence level for time series with 250 and 65 independent terms (degrees of freedom), respectively.

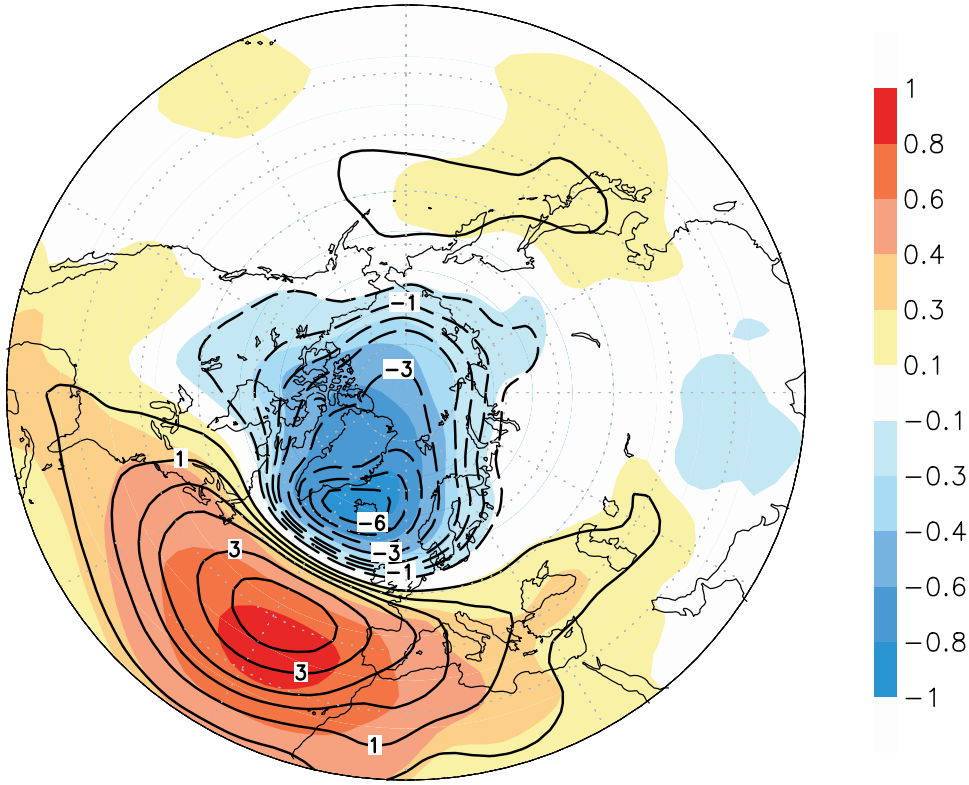

Figure 2. Correlation (shading)/regression (isolines) pattern between the standardized NAO index (Ponta Delgada (Azores)–Reykjavik (Iceland)) and the SLP based on the detrended monthly means of the extended cool season (November–April) for the period 1950–1998. The regression values are in hPa per one standard deviation of the NAO index. Negative contours are dashed and the zero contour line has been suppressed. Contour interval is 0.5 for absolute values smaller than 2.0 and 1.0 for absolute values greater than 2.0.

[15] The differences between Figures 2 and 3 (right) are coincident with the major differences between observations and simulations found by *Osborn et al.* [1999, Figure 3]. Clearly there is no significant correlation between the NAO index and SLP over the North Pacific when the stratospheric westerlies are weak (Figure 3, left).

[16] The significant correlation over the North Pacific in the SVR may give some explanation for the significant correlation between the PNA and the NAO, found in the above mentioned GCM simulation studies. The ECHAM4 model has a strong bias toward a too cold and strong polar vortex and therefore already in the mean tends to reflect the behavior that in the natural system only is observed for strong vortices. Figure 4 shows the frequency distribution of the daily 50 hPa zonal mean zonal wind at 65°N, for the ECHAM4 model in comparison with reanalyzed data, during the winter (DJF). *Hein et al.* [2001] found comparable results for an atmospheric model with higher resolution at the tropopause but still with an upper boundary at 10 hPa. Clearly, the bias of the model toward higher wind speeds is seen. Similar results were also found for models with a better representation of the stratosphere [*Pawson et al.*, 2000]. *Perlwitz and Graf* [2001a] showed with a single wave analysis (SWAN) of 10 day low-pass filtered NCEP reanalysis data from 1958 to 1999 for November–April that planetary waves of ZWN1 are refracted equatorward and downward at the strong westerlies in SVR, but not in WVR. In the WVR, ZWN1 generates wave disturbances in the stratosphere. In the SVR, the refraction of ZWN1 leads to tropospheric pressure anomalies of opposite signs over the North Atlantic and North Pacific.

[17] Since the pressure of the Icelandic Low is not in perfect anticorrelation with the Azores High, any physical interpretation may be complicated if the single centers of action each have their own specific contribution to the global field. We therefore also studied the regression/correlation of the North Atlantic centers of action sepa-

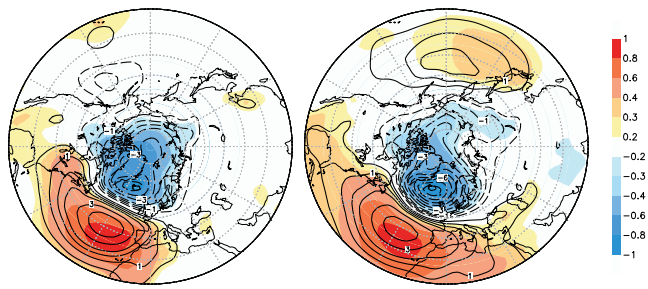

Figure 3. As in Figure 2, but considering (left) only the months with $0 < \overline{u}_{50}(65°\text{N}) < 10$ m s^{-1}, i.e., the WVR, and (right) only the months with $\overline{u}_{50}(65°\text{N}) > 20$ m s^{-1}, i.e., the SVR. Note that the minimum value of significant correlation was changed.

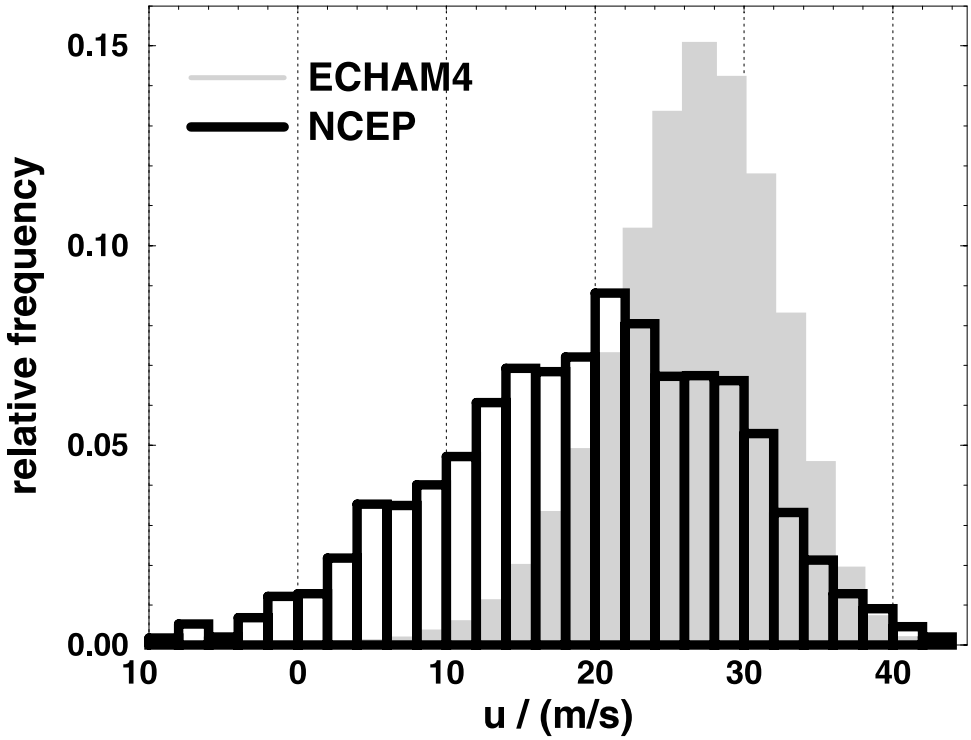

Figure 4. Frequency distribution of the daily 50 hPa zonal mean zonal wind at 65°N for the ECHAM4 model and NCEP reanalyzed data during the winter (DJF).

rately. Figure 5 (left and right) contains the analysis results for the WVR and the SVR, respectively, for the Azores High. In the subtropics there is a distinct difference between the two stratospheric regimes in the area of significant correlation of SLP with the Azores High. This area is smaller in the WVR and is extended over all North Africa in the SVR instead of being restricted to subtropical NW Africa as in the WVR. This already showed up in the analysis with the NAO index. Between 35°N and 45°N over the western North Pacific a positive correlation appears in the SVR which is not apparent in the WVR. It is found right where the in phase correlation between NAO and SLP is seen in Figure 3 (right), but is weaker both in correlation and in amplitude. Hence, here the Azores High is not the only contributor. The clearest differences between SVR and WVR exist over the North Atlantic and over the Arctic. In the SVR the connection between the Azores High and the Icelandic Low is much stronger (by a factor of 2 based on the regression over Iceland) and also the correlation is clearly different with maximum absolute correlation $|r|_{max}$ = 0.59 in the WVR versus $|r|_{max}$ = 0.67 in the SVR. The correlation/regression is very much concentrated on the Icelandic Low in the SVR, whereas it is much weaker and extended over the whole Arctic in the WVR.

[18] Figure 6 (left and right) shows the regression/correlation based on the Icelandic Low for the WVR and the SVR, respectively. Globally the two vortex regimes present the same differences as those mentioned above for the Azores High. However, in the SVR, the connection of the

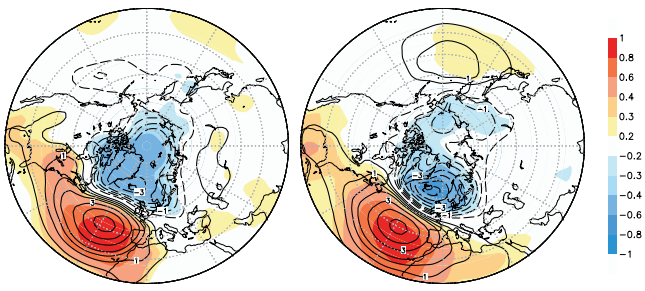

Figure 5. Correlation/regression patterns between the averaged pressure at four grid points near Ponta Delgada (Azores) and the SLP in the WVR (left) and SVR (right) cases. The four grid points considered are in the region where the correlation with the NAO index is maximum (see Figure 3). The maximum absolute correlation near Iceland is 0.59 and 0.67 in the WVR and SVR, respectively.

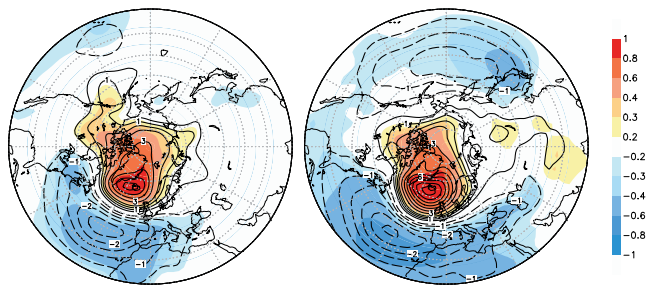

Figure 6. As in Figure 5, but considering four grid points near Reykjavik (Iceland). Contour interval is 0.5 for values smaller than 2.0 and 1.0 for values greater than 2.0. The maximum absolute correlation near Azores is 0.60 in the WVR (left) and 0.70 in the SVR (right).

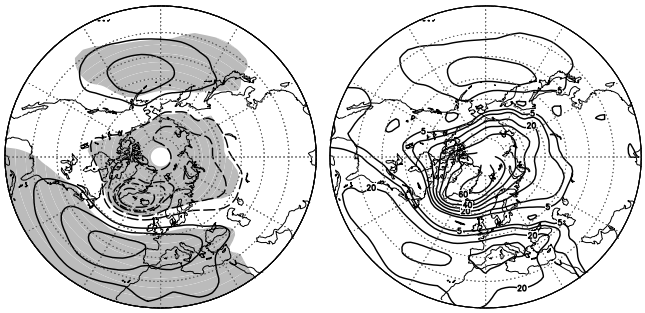

Figure 7. (a) Leading EOF of extended winter (November–April 1951–1998) monthly detrended SLP anomalies poleward of 20°N (19% of explained variance). The patterns have been obtained by regressing the monthly SLP anomalies upon the leading PC. Contour interval is 0.75 mb per standard deviation of the PC. The dashed-dotted contour is −2.5 mb/std. The shading shows regions where the PC explain more than 10% of local variance except for the Pacific where the local variance is above 5%. (b) Percentage of explained local variance by the leading PC. Contours are at intervals of 10 except for the 5% contour.

SLP over the North Pacific with the Icelandic Low (Figure 6, right) is stronger than the connection with the Azores High (Figure 5, right), as may be deduced from the respective regression/correlation maps.

[19] In all maps presented here, the regression coefficients have been normalized to the standard deviation of the time series onto which the regression is done. Hence, the squared regression coefficients represent the variance explained by the teleconnection patterns shown in each map. With this interpretation one can see that the SVR (Figure 6, right) is associated with a larger amount of SLP variance than the WVR (Figure 6, left).

[20] In order to see if smaller variance in the WVR may result from the large number of April months in the respective data subset, we repeated the analysis excluding the April months. There is no evidence that the main pattern features of the WVR may result from the large number of April months in the respective data subset.

[21] We analyzed the teleconnectivity of the three centers of the Arctic Oscillation (AO) pattern under different vortex regimes (SVR, WVR, and non-SVR) and for different definitions of the season (main winter months DJF, and extended winter November–April), using a procedure similar to the one of *Deser* [2000]. Figures 7a and 7b show the first EOF of detrended SLP north of 20°N and the fraction of local variance explained by the respective PC, considering the whole period November–April 1951–1998. Based on these patterns, we defined three detrended time series of averaged SLP anomalies for the Pacific, Atlantic and Greenland as follows: In the Pacific and the Atlantic centers the time series are given by the averaged area-weighted SLP anomalies over the regions inside the 0.75 hPa/std contours where the explained local variance is above 5% and 10%, respectively. Because of the large fraction of local variance explained over the Greenland sea, the third time series is given by the averaged area-weighted SLP anomalies inside the −2.5 hPa/std contour (see the dashed-dotted contour in Figure 7a). We refer to this time series as the Greenland SLP anomaly.

[22] The definition of the above three time series differs from the one of *Deser* [2000]. In our definition we tried to improve the signal-to-noise ratio excluding the regions where the explained local variance is small. Over the Pacific we chose a smaller threshold (5%) because the explained variance is smaller there (see Figure 7b). The three areas considered here are close to the three centers where *Honda et al.* [2001, Figure 5] found significant correlation. The resulting features of our calculations are not sensitive to the exact definition of the three centers.

[23] In Table 2, the correlations among detrended SLP anomaly times series of the Pacific, Atlantic and Greenland centers of action are given for the SVR, the non-SVR (i.e., for all months with zonal westerly winds at 50 hPa and 65°N smaller than 20 m s^{-1}), and the WVR. In the right part of the correlation matrices for the central winter months (DJF), in the left part for the extended period (November–April). The Atlantic–Greenland correlations are significantly negative (−0.67 to −0.71) in all cases, while significant correlations between Atlantic/Greenland with the Pacific center is only found in the SVR, but not in the non-SVR and WVR sub data sets. The significant SVR correlation between the Pacific center and Atlantic/Greenland is somewhat reduced when the extended winter period is used, but the general behavior of significant correlation in the SVR, but not in the non-SVR and WVR, is still valid. This also strengthens the argument that it is not the annual cycle of variability that determines our results, but instead supports our working hypothesis that it is certain critical zonal wind speeds in the lower stratosphere which determine the regime thresholds, independent of the months chosen. Computing the correlations between nondetrended SLP time series, we found the same general behavior of significant correlation in the SVR, but not in the non-SVR or WVR.

Table 2. Correlation Coefficients Among the Pacific, Atlantic, and Greenland Detrended Time Series of the Averaged Area-Weighted SLP Anomalies (See the Text for Definitions of the Time Series)[a]

	SVR			NSVR			WVR		
	Pac	Atl	Green	Pac	Atl	Green	Pac	Atl	Green
Pac	–	0.20*	−0.38**	–	−0.07	−0.07	–	−0.08	0.03
Atl	0.17*	–	−0.67**	−0.03	–	−0.71**	−0.03	–	−0.69**
Green	−0.35**	−0.67**	–	−0.04	−0.70**	–	0.00	−0.65**	–

[a]The values in the upper right of the matrix are for the main winter (December–February 1951–1998), and values in the lower left are for the extended winter (November–April 1951–1998). Values marked with an asterisk are above the 95% significance level without taking into account for serial autocorrelation. Values marked with two asterisks are above the 95% significance level, considering that only one-half of the months in each subset is independent for a conservative measure of the statistical significance.

Table 3. Interannual Correlation Between the February–March Mean SLP Anomalies of the Pacific and Greenland Centers[a]

	1951–1998			1951–1972			1973–1994		
	All data	SVW	NSVW	All data	SVW	NSVW	All data	SVW	NSVW
A	−0.26*	−0.52*	0.13	−0.10	−0.51	0.06	−0.52*	−0.91*	−0.39
B	−0.16	−0.37*	−0.02	−0.15	−0.61	0.02	−0.56*	−0.89*	−0.32
C	21/27			7/15			11/11		

[a]As explained in the text, the data were stratified according the vortex strength into Strong Vortex winter (SVW) and Nonstrong Vortex winter (NSVW). Values marked with an asterisk are above the 95% significance level. A ≡ detrended SLP, B ≡ not detrended SLP, C ≡ SVW/NSVW.

[24] It is after the International Geophysical Year (IGY) (1957/1958) that systematic rawinsonde observations of the NH stratosphere began. In order to see if the use of reanalyzed $\overline{u}$(50 hPa) for data stratification before 1957/1958 will affect our conclusions, we recalculated the correlations for the period after the winter 1957/1958. We obtained higher significant correlations between the North Atlantic/Greenland centers and North Pacific under SVR, but again no significant correlation for non-SVR or WVR.

[25] *Honda et al.* [2001] showed that the interannual variabilities of the Aleutian and Icelandic lows are anticorrelated. The ''peak period'' of anticorrelation is from 31 January to 16 March. As mentioned above, the centers of anticorrelation are very close to our Pacific and Greenland centers.

[26] Table 3 shows the interannual correlation between the February–March mean SLP anomalies of the Pacific and Greenland centers for the period 1951–1998, and two subperiods 1951–1972 and 1973–1994. Here, the data stratification between Strong and Nonstrong vortex is based not on the monthly means but on the main winter (DJF) mean zonal averaged 50 hPa zonal wind at 65°N. The subperiod 1973–1994 was analyzed by *Honda et al.* [2001] because they found a stronger anticorrelation during that period. We include in the table also the ratio of Strong Vortex to Nonstrong Vortex winters.

[27] Our data stratification based on the vortex strength seems to account well for the Honda et al. results. Strong Vortex winters show significant negative correlation between Pacific and Greenland, whereas Weak Vortex winters do not show such significant correlation. In the subperiod 1951–1972 Strong Vortex winters show a strong, but not significant, negative correlation due to the small number of Strong Vortex winters. Considering all data, a stronger negative correlation in the later subperiod may be due to the increase of the Strong to Nonstrong Vortex winters ratio.

4. Discussion

[28] We performed our analysis based on the hypothesis that there exist distinct regimes in northern winter atmospheric circulation. In one regime tropospheric vertically propagating planetary waves may enter the stratosphere, in the other not. The transition between the regimes would occur fast and produce nonlinear changes (as was shown by *Monahan et al.* [2001], (Monahan et al., submitted manuscript, 2001) with a nonlinear principal component analysis (NLPCA)). However, within the regimes linear variability modes may exist. Hence, we see the system as coupled of nonlinear variability (the regime transitions) with linear variability inside the regimes. The two branches found by *Monahan et al.* [2001], (Monahan et al., submitted manuscript, 2001) for the stratospheric modes in NLPCA may be interpreted as the regimes, while the regime internal variability is linear. Under this viewpoint of the regime nature of the dynamical link between tropospheric and stratospheric circulation, the NAO (defined as a linear variability mode) appears in both vortex regimes as an exact meridional seesaw of atmospheric mass over the North Atlantic. However, there are important differences between the two regimes. In the SVR, the meridional pressure gradient and the anomaly amplitudes over the North Atlantic are stronger, and the Azores High extends more over North Africa. Another important difference is the appearance of a significant correlation between the SLP over the NW Pacific and the NAO when the vortex is strong (Figure 3, right). The stratospheric winds thus control the North Atlantic–North Pacific relationship.

4.1. The North Pacific–North Atlantic Relationship

[29] The connection between the NAO and the North Pacific SLP is established in the SVR mainly through the Icelandic Low (see Figures 5 and 6 and Tables 2 and 3). This connection may result from an amplitude enhancement of ZWN1 in high latitudes, due to the tropospheric trapping of this wave by reflection at the strong zonal winds in the lower stratosphere. The statistical association of this teleconnection with the NAO (Figure 3, right) is dominated by the Icelandic Low and no underlying physical mechanism of the NAO is necessarily implied. As was shown by *Perlwitz and Graf* [2001a], in the WVR tropospheric planetary waves of ZWN1 will influence the stratospheric circulation but not vice versa. However, in the SVR a ZWN1 disturbance will exert an influence on the stratosphere and the stratospheric circulation acts back on the troposphere with maximum lag correlation at about 6 days. Figure 5 in the study of Perlwitz and Graf suggests that finally a tropospheric circulation anomaly results with opposite signs over Iceland and the Aleutians. The time lags of the linear correlation allow the conclusion that this process takes about 8–10 days and may, thus, be responsible for the quasi simultaneous anticorrelation in a monthly analysis.

[30] The results here obtained for the SVR also suggest that the result of *Osborn et al.* [1999], *May and Bengtsson* [1998], and Ulbrich and Christoph (submitted manuscript, 2002), which shows a connection between the NAO and North Pacific SLP simulated by the HadCM2 and the ECHAM model family, may be due to a bias of the planetary waves refraction index in the simulated upper troposphere–lower stratosphere. This may be the case for the ECHAM model due to its strong vortex bias. However,

the HadCM2 shows a warm polar bias in the polar stratosphere in winter and an equatorward shift of the polar jet [*Johns et al.*, 1997]. Obviously other factors, like a smaller vertical gradient of zonal wind near the tropopause [*Hu and Tung*, 2002] may contribute for a bias in planetary waves refraction index, for this specific model. Further studies are certainly needed to understand the model behavior.

4.2. The Pattern of the NAO and Regime Transitions

[31] Based on our results, the patterns obtained in linear studies (in our interpretation those that do not separate between different stratospheric regimes) must be influenced by the difference between the mean tropospheric circulation in the two vortex regimes. Figure 8 presents the difference between the mean SLP fields of the two vortex regimes (SVR–WVR). Statistically significant (local t-test) negative differences appear mainly north of the Polar Circle, and in the midlatitudes over the Euro-Atlantic region significant positive differences are found. Negative anomalies extending over the whole polar cap imprint a zonal character to the difference pattern [*Deser*, 2000]. However, very contrasting pressure gradients are found over the North Pacific and the North Atlantic. A much stronger pressure gradient representing a SW-NE tilt of streamlines is observed over the Euro-Atlantic region. This feature compares well with Figure 5a in the study of *Perlwitz and Graf* [1995]. The SW-NE streamline tilting is also shown in Figure 3c (left-hand column) in the study of *Kodera et al.* [1999]. We are aware that in this study we are considering an extended winter (November–April), while the above cited authors considered only the months of December–February. However, Figure 8 compares also well with Figure 2 (middle) in the study of *Deser* [2000] and with Figure 7c in the study of *Perlwitz and Graf* [2001b] who used the same extended cool season. Concerning the teleconnectivity, Table 2 indicates that the specific months do not make a significant difference.

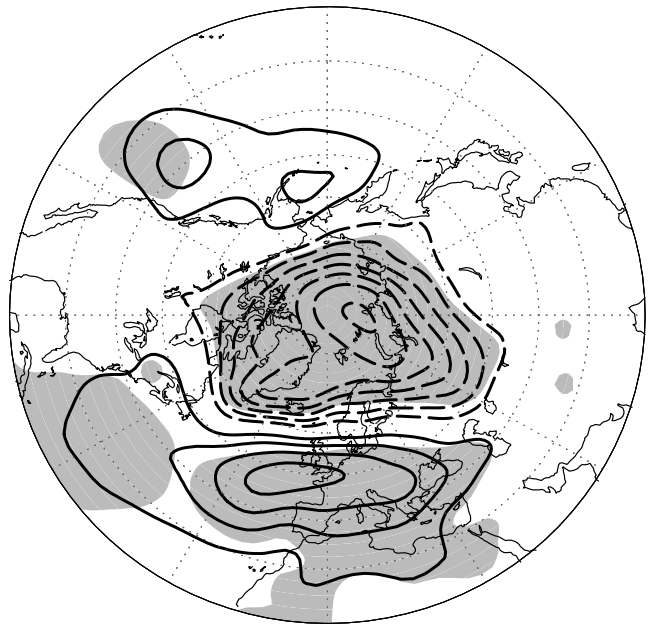

Figure 8. Difference between the mean SLP in the two vortex regimes (SVR–WVR). Contour interval is 0.75 mb. Negative contours are dashed and the zero contour line has been suppressed. The shading indicates where the mean difference is significant at least at the 95% confidence level.

[32] Our Figure 8 compares also fairly well with the EOF pattern of SLP presented by *Thompson and Wallace* [1998, Figures 1 and 2], a pattern that was named "Arctic Oscillation." As already discussed, this AO pattern has a more zonal character (mainly due to the Arctic center) [*Deser*, 2000] than that shown by the NAO patterns presented here. The AO pattern, which is most clearly defined near the surface (SLP) must be influenced by the difference of the mean pressure of the two regimes over the Northern Hemisphere. Since the AO pattern now can be interpreted as the difference of the mean states of the troposphere (not only of the surface pressure field!) during times of preferred strong and weak polar vortex, it may not necessarily represent a physical mode of tropospheric variability alone. It was interpreted by *Monahan et al.* [2001], (Monahan et al., submitted manuscript, 2001) as the mode resulting from the transition between two stable stratospheric regimes. *Hartley et al.* [1998] and *Black* [2002] suggested an adjustment of the tropospheric zonal wind field to an initial stratospheric forcing induced by stratospheric Potential Vorticity (PV) anomalies and subsequent downward propagation. *Ambaum and Hoskins* [2002] showed that an SVR Arctic low center may result of tropopause lifting following geostrophic adjustment to positive PV anomalies. The AO index then represents variance due to stratospheric vortex regime changes, which are picked up as the leading coherent pattern of variability if simple EOF analysis is applied. This is due to the fact that the downward propagating stratospheric signal has a longer timescale and exists mainly in just two polarities. In contrast tropospheric variability has shorter timescales, a much higher degree of freedom and less coherent structures due to the many different processes producing this variability [*Perlwitz and Graf*, 2001b]. For very strong stratospheric anomalies of both signs, *Baldwin and Dunkerton* [2001] recently even suggested the possibility of forecasting tropospheric weather over several weeks.

[33] As mentioned above, the NAO patterns obtained in our study are characterized by a strictly meridional dipole in both vortex regimes. The same orientation was found by *Kodera et al.* [1999, Figure 3b] for the NAO with the linear influence of the polar vortex removed by regression. In three-dimensional linear analyses (e.g., CCA or SVD) of coupled stratospheric and tropospheric circulation variability [*Perlwitz and Graf*, 1995, 2001b; *Kodera et al.*, 1999; *Deser*, 2000; *Castanheira et al.*, 2002] that account for vertical planetary wave propagation, the obtained patterns must also be influenced by the mean difference as well as by the differences in the teleconnection mechanisms operating under each vortex regime, leading to the typical SW-NE tilt of the node line of the coupled tropospheric pattern over the Euro-Atlantic region. Hence, our results suggest that linear analysis, i.e., the neglect of the existence of different regimes of planetary wave propagation, may lead to a mix of dynamical features with the mean state of the different regimes. Only taking into account the nonlinear transition between the regimes, as done here or in NLPCA by

Monahan et al. [2001], (Monahan et al., submitted manuscript, 2001) will allow for the isolation of variability mechanisms.

5. Conclusions

[34] Our analysis showed that stratospheric circulation controls the correlation between the North Atlantic and the North Pacific pressure patterns at least in a statistical sense. A teleconnection between SLP over the North Pacific and the North Atlantic is found during the SVR, but not when the polar vortex is weak (WVR) or just does not exceed the limit of 20 m s^{-1} at 50 hPa near the polar circle.

[35] Another significant result of our analysis concerns the pattern structure of the NAO. If the analysis takes into account that strong and weak polar vortex represent two different regimes of atmospheric circulation, the NAO pattern appears as a strict meridional dipole. This result corresponds with findings of *Castanheira et al.* [2002] that an NAO-like strictly meridional dipole over the North Atlantic is an Eigensolution of the equations of motion linearized around a layered atmosphere at rest. However, some differences in the correlation/regression patterns are observed between the two stratospheric vortex regimes. The teleconnection over the North Atlantic appears to be stronger during the SVR and the Azores High extends farther over North Africa.

[36] The difference between the mean SLP fields of the two vortex regimes (Figure 8) shows a spatial structure close to that of the first EOF of SLP when computed over the whole extratropical Northern Hemisphere [*Thompson and Wallace*, 1998], the AO pattern. This pattern was interpreted by *Monahan et al.* [2001], (Monahan et al., submitted manuscript, 2001) as a transitional mode between two hemispheric variability regimes, based on NLPCA. The characteristic SW to NE tilt of the isobars over the Euro-Atlantic region, found in these patterns, is also obtained when the SLP EOF is computed only over the Euro-Atlantic region in winter [*Glowienka-Hense*, 1990]. The same result may be obtained from three-dimensional linear studies of the coupled lower stratospheric and tropospheric circulation variability [*Perlwitz and Graf*, 1995, 2001b; *Kodera et al.*, 1999; *Deser*, 2000; *Castanheira et al.*, 2002]. In all these studies the NAO patterns over the Euro-Atlantic region are oriented in the same way in winter: SW-NE. However, the similarity of those patterns with the mean difference pattern between the two vortex regimes obtained here (Figure 8) suggests that the linear statistical methods that were usually applied may be sensitive to a mix of different dynamical mechanisms: The fast transitions between stratospheric circulation regimes and the vertical propagation of barotropic Rossby waves. This result has important consequences if the internal mechanisms and the external forcings leading to changes between the two vortex regimes are different and/or they operate largely independent from those which determine the strength of the N-S oriented NAO. In this case we must study the forcings of the meridional NAO separately during the WVR (or just non-SVR) and the SVR.

[37] **Acknowledgments.** We thank José Silvestre for providing us with Figure 4. This work was partially sponsored by the Max-Planck-Society and by BMBF under the project PROVAM in AFO2000/KODYACS and by the Portuguese Science Foundation (FCT) under the project POCTI/CTA/38326/2001.

References

Ambaum, M. H. P., and B. J. Hoskins, The NAO troposphere–stratosphere connection, *J. Clim.*, *15*, 1969–1978, 2002.

Ambaum, M. H. P., B. J. Hoskins, and D. B. Stephenson, Arctic Oscillation or North Atlantic Oscillation?, *J. Clim.*, *14*, 3495–3507, 2001.

Andrews, D. G., J. R. Holton, and E. C. B. Leovy, *Middle Atmosphere Dynamics*, 489 pp., Academic, San Diego, Calif., 1987.

Baldwin, M. P., and T. J. Dunkerton, Stratospheric harbingers of anomalous weather regimes, *Science*, *294*, 581–584, 2001.

Barnett, T. P., Variations in near-global sea level pressure, *J. Atmos. Sci.*, *42*, 478–501, 1985.

Black, R. X., Stratospheric forcing of surface climate in the Arctic Oscillation, *J. Clim.*, *15*, 268–277, 2002.

Castanheira, J. M., H.-F. Graf, C. DaCamara, and A. Rocha, Using a physical reference frame to study Global Circulation Variability, *J. Atmos. Sci.*, *59*, 1490–1501, 2002.

Charney, J. G., and P. G. Drazin, Propagation of planetary-scale disturbances from the lower into the upper atmosphere, *J. Geophys. Res.*, *66*, 83–109, 1961.

Corti, S., F. Molteni, and T. N. Palmer, Signature of recent climate change in frequencies of natural atmospheric regimes, *Nature*, *398*, 799–802, 1999.

Deser, C., On the teleconnectivity of the "Arctic Oscillation", *Geophys. Res. Lett.*, *27*, 779–782, 2000.

Glowienka-Hense, R., The North Atlantic Oscillation in the Atlantic–European SLP, *Tellus*, *42A*, 497–507, 1990.

Hartley, D. E., J. Villarin, R. X. Black, and C. A. Davis, A new perspective on the dynamical link between the stratosphere and troposphere, *Nature*, *391*, 471–474, 1998.

Hartmann, D. L., J. M. Wallace, V. Limpasuvan, D. W. J. Thompson, and J. R. Holton, Can ozone depletion and global warming interact to produce rapid climate change?, *Proc. Natl. Acad. Sci. U.S.A.*, *97*, 1412–1417, 2000.

Hein, R., et al., Results of an interactively coupled atmospheric chemistry: General circulation model: Comparison with observations, *Ann. Geophys.*, *19*(4), 435–457, 2001.

Honda, M., H. Nakamura, J. Ukita, I. Kousaka, and K. Takeuchi, Interannual seesaw between the Aleutian and Icelandic lows, part 1, Seasonal dependence and life cycle, *J. Clim.*, *14*, 1029–1042, 2001.

Hu, Y., and K. K. Tung, Interannual and decadal variations of planetary wave activity, stratospheric cooling, and Northern Hemisphere Annular Mode, *J. Clim.*, *15*, 1659–1673, 2002.

Johns, T. C., et al., The second Hadley Centre coupled ocean–atmosphere GCM: Model description, spinup and validation, *Clim. Dyn.*, *13*, 103–134, 1997.

Kalnay, E., et al., The NCEP/NCAR 40-year reanalysis project, *Bull. Am. Meteorol. Soc.*, *77*, 437–471, 1996.

Kodera, K., H. Koide, and H. Yoshimura, Northern Hemisphere winter circulation associated with the North Atlantic Circulation and the stratospheric polar-night jet, *Geophys. Res. Lett.*, *26*, 443–446, 1999.

Latif, M., K. Arpe, and E. Roeckner, Oceanic control of decadal North Atlantic sea level pressure variability, *Geophys. Res. Lett.*, *27*, 727–730, 2000.

May, W., and L. Bengtsson, The signature of ENSO in the Northern Hemisphere midlatitude seasonal mean flow and high-frequency intraseasonal variability, *Meteorol. Atmos. Phys.*, *69*, 81–100, 1998.

Monahan, A. H., L. Pandolfo, and J. C. Fyfe, The preferred structure of variability of the Northern Hemisphere atmospheric circulation, *Geophys. Res. Lett.*, *28*, 1019–1022, 2001.

Osborn, T. J., K. R. Briffa, S. F. B. Tett, P. D. Jones, and R. M. Trigo, Evaluation of the North Atlantic Oscillation as simulated by a coupled climate model, *Clim. Dyn.*, *15*, 685–702, 1999.

Paeth, H., et al., The North Atlantic Oscillation as an indicator for greenhouse-gas induced regional climate change, *Clim. Dyn.*, *15*, 953–960, 1999.

Palmer, T. N., A nonlinear dynamical perspective on climate prediction, *J. Clim.*, *12*, 575–591, 1999.

Pawson, S., et al., The GCM-reality intercomparison project for SPARC (GRIPS): Scientific issues and initial results, *Bull. Am. Meteorol. Soc.*, *81*, 781–796, 2000.

Perlwitz, J., and H.-F. Graf, The statistical connection between tropospheric and stratospheric circulation of the Northern Hemisphere in winter, *J. Clim.*, *8*, 2281–2295, 1995.

Perlwitz, J., and H.-F. Graf, Troposphere–stratosphere dynamic coupling under strong and weak polar vortex conditions, *Geophys. Res. Lett.*, *28*, 271–274, 2001a.

Perlwitz, J., and H.-F. Graf, The variability of the horizontal circulation in the troposphere and stratosphere: A comparison, *Theor. Appl. Clim.*, *69*, 149–161, 2001b.

Perlwitz, J., H.-F. Graf, and R. Voss, The leading variability mode of the coupled troposphere–stratosphere winter circulation in different climate regimes, *J. Geophys. Res.*, *105*, 6915–6926, 2000.

Randel, W. J., D. S. Stevens, and J. L. Stanford, A study of planetary waves in the Southern winter troposphere and stratosphere, part 2, Life cycles, *J. Atmos. Sci.*, *44*, 936–949, 1987.

Rodwell, M. J., D. P. Rowell, and C. K. Folland, Oceanic forcing of the wintertime North Atlantic Oscillation and European climate, *Nature*, *398*, 320–323, 1999.

Thompson, D. W., and J. M. Wallace, The Arctic Oscillation signature in the wintertime geopotential height and temperature fields, *Geophys. Res. Lett.*, *25*, 1297–1300, 1998.

J. M. Castanheira, Department of Physics, University of Aveiro, 3810-193, Aveiro, Portugal. (jcast@fis.ua.pt)

H.-F. Graf, Max-Planck Institute for Meteorology, Hamburg, Germany.